Journal of Applied Polymer Science

Kinetic and thermodynamic control in conductive PP/PMMA/EAA carbon black composites

Paul J. Brigandi,[1,2] Jeffrey M. Cogen,[1] Casey A. Wolf,[1] John R. Reffner,[1] Raymond A. Pearson[2]
[1]The Dow Chemical Company, 400 Arcola Road, Collegeville, Pennsylvania 19426-2914
[2]Center for Polymer Science and Engineering, Lehigh University, Bethlehem, Pennsylvania 18015-3195
Correspondence to: P. J. Brigandi (E-mail: pjbrigandi@dow.com)

ABSTRACT: Multiphase polymer blends provide unique morphologies to reduce the percolation concentration and increase conductivity of carbon-based polymer composites via selective distribution of the conductive filler. In this work, the kinetic and thermodynamic effects on a series of multiphase conductive polymer composites were investigated. The electrical conductivity of carbon black (CB)-filled conductive polymer blend composites comprising polypropylene, poly(methyl methacrylate), and ethylene–acrylic acid were determined as a function of compounding sequence and annealing time. Kinetic and thermodynamic parameters were found to influence the conductivity. Phase morphology and conductivity at short annealing times were influenced by the compounding sequence where the CB was added after being premixed with one of the polymer components or directly added to the three-component polymer melt. However, they were thermodynamically driven at longer annealing times; the resistivity was found to decrease by a statistically significant amount to similar levels for all the composite systems with increasing annealing time. The increase in conductivity at longer annealing times was determined to be the result of changes in the phase morphology from sea-island, dispersed microstructure to a tri-continuous morphology rather than change in localization of CB, given that the CB was found to be entirely located in the EAA phase even at short annealing times (and independent of compounding sequence), where the conductivity was not measurable. © 2015 Wiley Periodicals, Inc. J. Appl. Polym. Sci. **2015**, *132*, 42134.

KEYWORDS: blends; composites; dielectric properties; morphology

Received 26 April 2014; accepted 20 February 2015
DOI: 10.1002/app.42134

INTRODUCTION

Electrically conductive polymer composites (CPC) consisting of conductive filler such as carbon black (CB), carbon nanotubes (CNT), or graphene dispersed in a polymer system continue to attract increasing academic and industrial research. CPCs are used in a wide range of industrial applications such as antistatic and electrostatic dissipation materials, positive temperature coefficient materials, electromagnetic interference shielding,[1] and semiconducting layers in power cables to provide a uniform voltage stress over the conductor and close bonding between the conductor and insulation to prevent partial discharge.[2]

In general, single polymer systems require a substantial concentration of conductive filler to achieve significant electrical conductivity on the order of 10^{-9} to 10^{-3} S/cm, which increases the melt viscosity and decreases the mechanical properties of the material.[3] One approach to increase composite conductivity at reduced filler concentrations and minimize detrimental impact on mechanical and rheological properties is to use multiphase polymer blends that can reduce the percolation threshold.[4–7] For the case of a two-component polymer blend, this has often been referred to as double percolation. Double percolation is governed by the percolation of the CB-rich phase and the continuity of this phase in the polymer blend. Several studies found that the percolation threshold has been reduced using multiphase polymer systems where the conductive filler was incorporated into immiscible polymer blends.[8–10]

The percolation threshold in binary polymer blends depends on the phase morphology and distribution of conductive filler. The conductive filler tends to partition in one of two ways that benefits electrical conductivity at reduced loading, the first being where the conductive filler is distributed predominantly in one continuous phase and the other where the conductive filler is located preferentially at the interface between the two polymer phases. The selective localization of the conductive filler at the interface provides the CPC with the lowest filler loading if the interfacial region is continuous. The kinetic and thermodynamic factors that influence the selective distribution of conductive fillers in polymer blends include the co-continuity of the polymer blend, affinity of conductive filler to different polymers,[11]

Table I. Properties of the Polymers Used in This Study

Material	Product	Supplier	MFI (g/10 min)	Density (g/cm^3)
Polypropylene	FF018F	Braskem	1.8[a]	0.905
Poly(methyl methacrylate)	IF 850B	LG Chemical	12.1[b]	1.180
Ethylene–acrylic acid copolymer	Primacor 3004	Dow Chemical	8.5[c]	0.938

[a] ASTM D 1238 (230°C, 2.16 kg).
[b] ASTM D 1238 (230°C, 3.8 kg).
[c] ASTM D 1238 (190°C, 2.16 kg).

interfacial tension between components of the composite,[12,13] melt viscosity ratios of the polymers,[14] mixing time and temperature, and sequence of incorporation.[15]

Triple percolation is a more recent approach to reduce the percolation threshold in CPC. The concept of triple percolation utilizes a ternary polymer blend in combination with conductive filler. Virgilio *et al.*[16] suggested existence of four different morphologies of a ternary blend comprised of two major phases and one minor phase, depending on the values of the three spreading coefficients calculated based on the surface tension and interfacial tension of the individual components. Al-Saleh and Sundararaj[17–19] reported a 40% reduction in the percolation threshold of immiscible polypropylene (PP)/polystyrene (PS)/CB blends by introduction of a styrene–butadiene–styrene (SBS) triblock copolymer as a result of the high affinity of CB to the butadiene block of SBS copolymer, which was selectively localized at the interface between the PP and PS phases. Lu *et al.*[20,21] reported selective localization of CB at the interface of polymer blends by compatibilization with poly(styrene-*co*-maleic anhydride) (SMA) that was first reacted with the CB and then blended with polyamide (PA6)/PS. In the PA6/PS blends, CB was localized in the PA6 phase and typical double percolation was exhibited, whereas in the PA6/PS/(SMA–CB) blends, TEM results showed that CB particles were induced by SMA to localize at the interface, resulting in a very low percolation threshold.

Shen *et al.*[22] studied thermodynamically induced self-assembled electrically conductive networks consisting of a ternary blend system of poly(methyl methacrylate) (PMMA), ethylene–acrylic acid copolymer (EAA), and PP, building on extensive results in related CPC materials based on binary polymer blends.[23–25] It was proposed that the system formed a tri-continuous "sandwich-like" phase structure, in which PMMA and PP formed a co-continuous phase and the EAA, which was premixed with CB, spread at the interface of the PMMA and PP. The percolation threshold of the PMMA/EA–CB/PP composites was one-fifth that of PP/CB composites. Achieving conductivity at very low CB levels and based on readily available raw materials, Shen's ternary blend composites offer potential for use in practical applications requiring CPC materials. However, with post-compounding annealing times of 30 min, it is of interest to explore and understand alternative strategies for preparation of these composites.

To that end, this study aimed at understanding how kinetic and thermodynamic factors may be utilized to influence the conductivities in such systems. This article demonstrates how different annealing times influence the polymer blend phase morphology and localization of filler to increase electrical conductivity. Effects of compounding sequence and thermal annealing time on conductivity in CB-filled PP/PMMA/EAA conductive polymer blend composites were explored. Such knowledge will be useful to expand understanding of factors affecting performance in these systems and is essential toward development of an efficient process for making them.

EXPERIMENTAL

Materials

Three polymers were used as matrix resins in the preparation of ternary polymer blends. The polymers included PP from Braskem, PMMA from LG Chemicals, and EAA copolymer with 9.7 wt % acrylic acid from Dow Chemical, which were used as received. Properties of the polymers are summarized in Table I. The conductive filler was Ketjenblack EC-300J extra-conductive CB from Akzo Nobel, which was used as received. This grade of CB has a high surface area of 800 m^2/g and pore volume (or structure) of 327 mL/100 g.

Formulations

A series of CPC prepared with different CB masterbatches and compounding sequences was studied. PP/PMMA/EAA multiphase polymer blends were chosen as a starting point based on the work by Shen *et al.*,[22] which suggested that the PP and PMMA form a co-continuous morphology with the EAA phase sandwiched at the interface. In Shen's study, the CB was premixed at 3.2 vol % in the EAA phase before preparing the composites so that the conductive filler would be preferentially distributed in the EAA phase at the PP/PMMA interface to achieve conductivity at a low level.

In this work, the PP/PMMA/(EAA–CB) formulation was prepared as a starting point similar to compositions studied by Shen. In the PP/(PMMA–CB)/EAA and (PP–CB)/PMMA/EAA formulations the CB was premixed into the PMMA and PP phases, respectively, while the PP/PMMA/EAA/CB formulation was prepared by direct addition of CB during the melt mixing process, with CB and polymer levels selected to provide the same nominal formulations for all compositions evaluated (Tables II and III). These formulations enable assessment of kinetic and thermodynamic factors by comparing how the mode of CB addition and annealing time impact the composite conductivity.

Melt Compounding

The masterbatches and composites were melt-mixed using an internal C.W. Brabender prep-mixer. Two different procedures

Table II. Conductive Polymer Composite Formulations Used in This Study

Composite (vol %)	PP/PMMA/(EAA–CB)	PP/(PMMA–CB)/EAA	(PP–CB)/PMMA/EAA	PP/PMMA/EAA/CB
PMMA	42.0		42.0	42.0
PP	42.0	42.0		42.0
EAA		15.5	15.5	15.5
PMMA–CB		42.5		
PP–CB			42.5	
EAA–CB	16.0			
CB				0.5

were used for the preparation of the masterbatches and composites. For the masterbatches, the CB and polymer were directly compounded at 35 rpm for 5 min at 130°C for the EAA–CB and 190°C for the PMMA and PP–CB samples. For the multiphase composites, the CB or CB masterbatches were mixed with base resins (PP and/or EAA and/or PMMA) and compounded at 190°C at 60 rpm for 5 min.

Thermal Annealing

The polymer composites were compression molded at 190°C and 3.45 MPa for 3 min before testing. After 3 min, the pressure was increased to 17 MPa followed by thermal annealing at 190°C for 6, 30, and 150 min.

Morphology

Samples were excised from plaques in 1 cm × 1 cm squares and trimmed down with a razor blade to have a block face roughly <0.5 mm × 0.5 mm. These rough block faces were then polished with a Diatome Cryo 45 Trim knife, stained in a 0.5% RuO_4 solution for 16 h, and then rinsed with DI water. For TEM, 70–100 nm thick sections were then cut from the stained block face using a Leica UC7 microtome at room temperature with a Diatome Sonic knife (voltage: 2.1, frequency: 33.4 Hz) and collected on Formvar-coated TEM grids. TEM images were obtained with a Hitachi 7000 at 125 keV. SEM samples were prepared by removing roughly 1 μm from the block face using a Diatome Cryo 45 Trim knife. The faces were then sputter coated with about 10 nm Au/Pd. SEM images were obtained with a Hitachi 3400 in variable pressure mode using a backscatter detector. Solvent etching of block faces was done by submerging samples in tetrahydrofuran (THF) for 18 h, rinsing the samples off with THF two times, drying at room temperature, and then sputter coating with Au/Pd. Solvent-etched samples were imaged with a secondary electron detector.

Electrical Resistivity

Electrical resistivity measurements were conducted using a Keithley 2700 Integra Series digital multimeter with two-point probe. At least two samples (101.6 mm long by 50.8 mm wide by 1.9 mm thick) were tested for each formulation. The electrical resistivities of the polymer composites were obtained from compression-molded samples. Silver paint (conductive silver #4817N) was applied to minimize contact resistance between the samples and electrodes. Resistivity values were measured at various temperatures in Blue M air convection ovens using a multimeter.

Rheology

Dynamic oscillatory shear rheology was conducted with an ARES oscillatory shear rheometer for analysis of viscoelastic behavior. The oscillatory shear measurements were conducted at 190°C with the parallel plate geometry (plate diameter of 25 mm). Frequency sweeps were carried out at 2% strain between a frequency of 0.1 and 100 rad/s. The strain was chosen within the linear viscoelastic region.

RESULTS AND DISCUSSION

The theory and models to predict polymer blend phase morphology are predominately based on thermodynamic parameters where thermodynamic control should occur spontaneously and becomes effective at thermodynamic equilibrium; however, in practice, each conductive polymer blend composite system is a case in itself that requires specific optimization. The kinetic factors cannot be ignored in real systems and often have a large impact in determining arrangement of conductive fillers in the polymer matrix. The balance of the interactions of the filler with each constitutive polymeric component may control the CB distribution in binary or ternary polymer blends. However, thermal annealing at elevated temperatures may accelerate the structural evolution of the percolation network and the phase morphology in CB-filled polymer blends.

It should be pointed out that in this work kinetic control refers to a nonequilibrium state that exists as a result of the method used to prepare the composites, including compounding method and any postcompounding treatment, such as annealing, whereas thermodynamic control refers to the state that is achieved as the system approaches equilibrium.

Electrical Resistivity

A CB level of 0.5 vol % was selected for this study based on the fact that this level was found to be comfortably above the percolation threshold yet still at an efficiently low level compared

Table III. Premixed Masterbatch Formulations Used in This Study

MB (vol %)	EAA–CB	PP–CB	PMMA–CB
PMMA			98.8
PP		98.8	
EAA	96.8		
CB	3.2	1.2	1.2

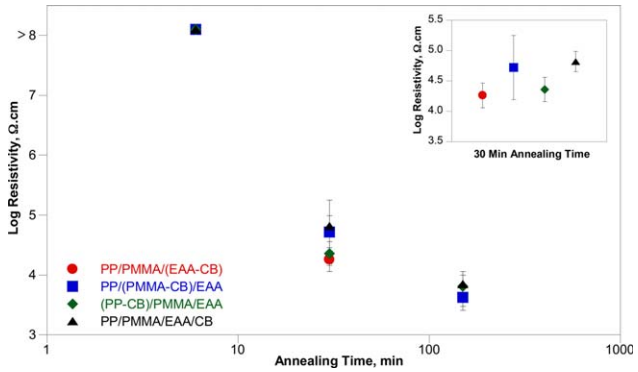

Figure 1. Resistivity at room temperature as a function of annealing time of the multiphase composites. The inset plots resistivity with error bars showing ±1 standard deviation after annealing for 30 min. [Color figure can be viewed in the online issue, which is available at wileyonlinelibrary.com.]

to single-phase CPCs. The conductivity data for the four different compositions after 0, 30, and 150 min of annealing time are shown in Figure 1. The log of resistivity for the 0.5 vol % CB PP/PMMA(EAA–CB) sample after 30 min of annealing time at 190°C in this work (value of ~4.2 Ω-cm from Figure 1) matches well with the value obtained by Shen *et al.*[22]

Room Temperature Resistivity as a Function of Annealing. As previously mentioned, the conductive multiphase composites were prepared by introducing the CB premixed within one of the three polymer phases as well as directly (neat) during the melt compounding. The evolution of CB distribution in the multiphase system was investigated by thermal annealing under high pressure following the intensive melt compounding. The room temperature resistivity as a function of annealing time was the main property of interest. Therefore, each blend was prepared and evaluated in duplicate in order to be able to assess the resulting reproducibility of compounding and resistivity. Figure 1 shows the room temperature resistivity as a function of annealing time for the composite systems with 0.5 vol % CB.

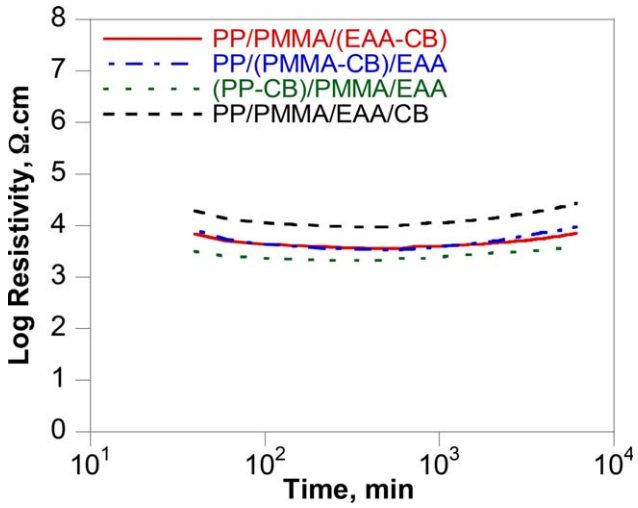

Figure 2. Resistivity at 160°C as a function of time for the multiphase composites annealed at 190°C for 30 min. [Color figure can be viewed in the online issue, which is available at wileyonlinelibrary.com.]

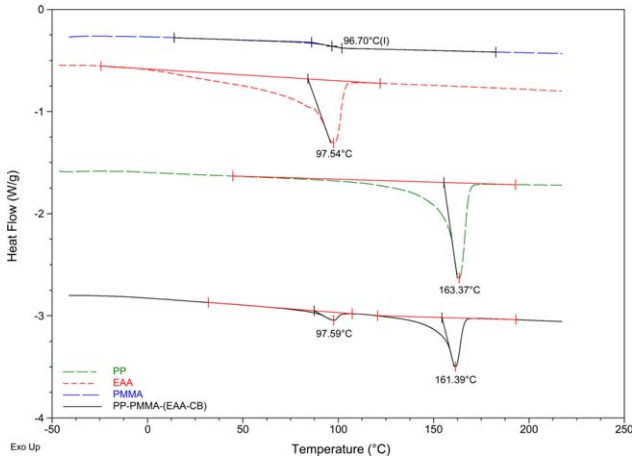

Figure 3. DSC thermograms for the individual polymers and the PP/PMMA/(EAA–CB) ternary polymer blend composite in the temperature range of −50 to 220°C. [Color figure can be viewed in the online issue, which is available at wileyonlinelibrary.com.]

The composites were annealed at 190°C under a pressure of 17 MPa for 6, 30, and 150 min. It was found that the resistivities of all the composites after 6 min annealing exceeded the measurement capability and therefore had a resistance greater than about 1.2×10^8 Ω (volume resistivity $> 7.4 \times 10^7$ Ω-cm for these specific samples). Clearly, the kinetically determined morphology during mixing followed by only a 6 min annealing at 190°C does not result in a favorable conductivity (Figure 1).

The resistivity was found to decrease significantly with increasing annealing time, consistent with gradual phase coalescence to the thermodynamically favorable highly conductive tri-continuous morphology proposed previously.[22] After 30 min of annealing, the data suggest that the resistivities of the PP/PMMA/(EAA–CB), PP/(PMMA–CB)/EAA–CB, and (PP–CB)/PMMA/EAA are all the same, within experimental error and

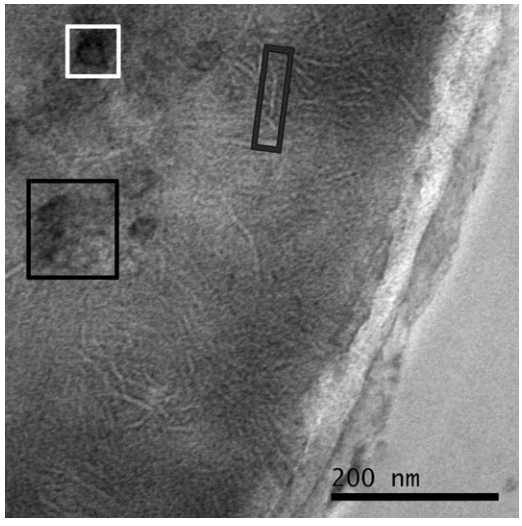

Figure 4. TEM image showing CB morphology. The white box surrounds an individual CB particle and the black box indicates an area with several agglomerated CB particles. The gray rectangle surrounds one of the crystalline lamellae formed by EAA.

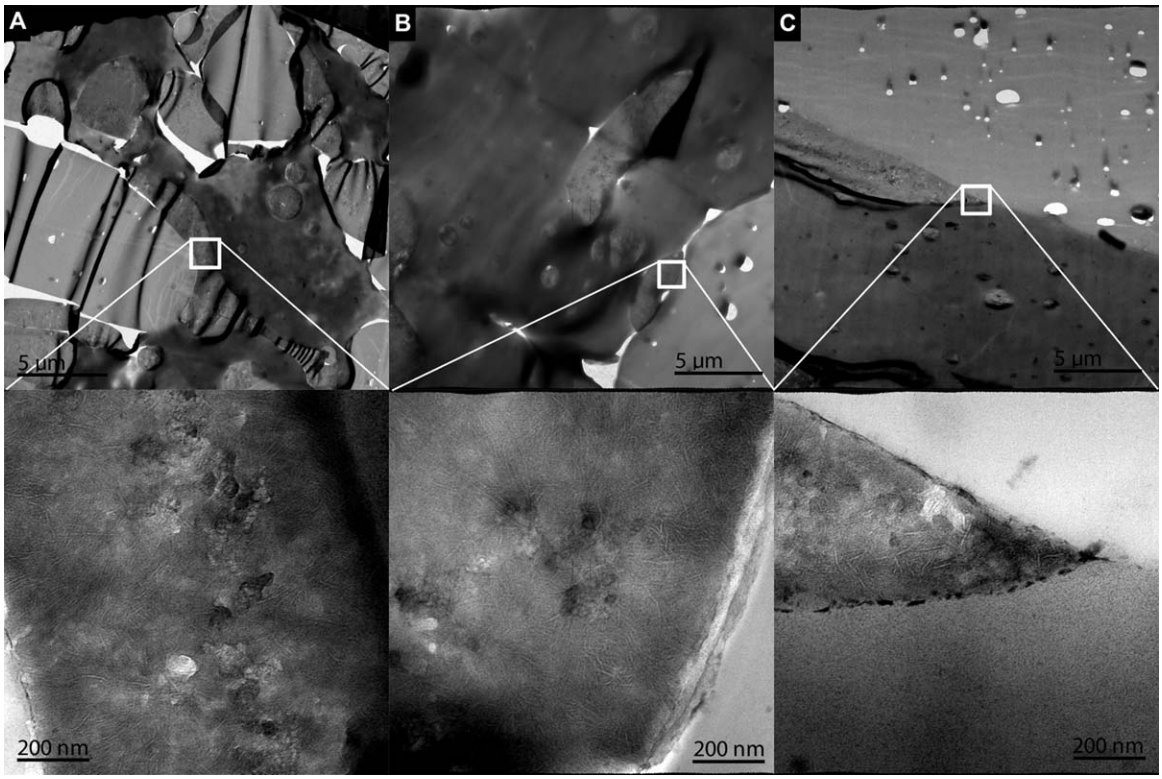

Figure 5. TEM images of PP/PMMA/(EAA–CB) annealed for (A) 6 min, (B) 30 min, and (C) 150 min. Top row shows images for each annealing time at 1000× magnification. Bottom row (20,000× magnification) shows CB (~20 nm bright spots with dark edges in the EAA phase) as well as the semicrystalline structure of the EAA.

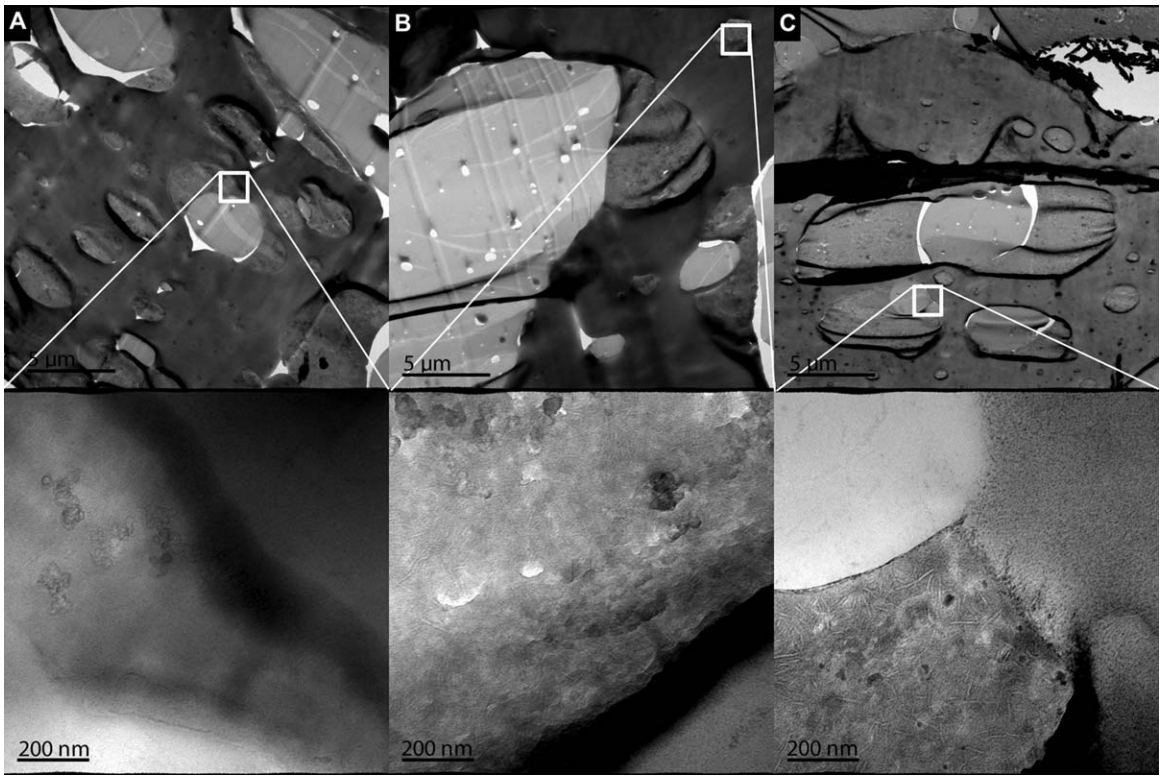

Figure 6. TEM images of PP/PMMA/EAA/CB annealed for (A) 6 min, (B) 30 min, and (C) 150 min. Top row shows images for each annealing time at 1000× magnification. Bottom row (20,000× magnification) shows CB (~20 nm bright spots with dark edges in the EAA phase) as well as the semicrystalline structure of the EAA.

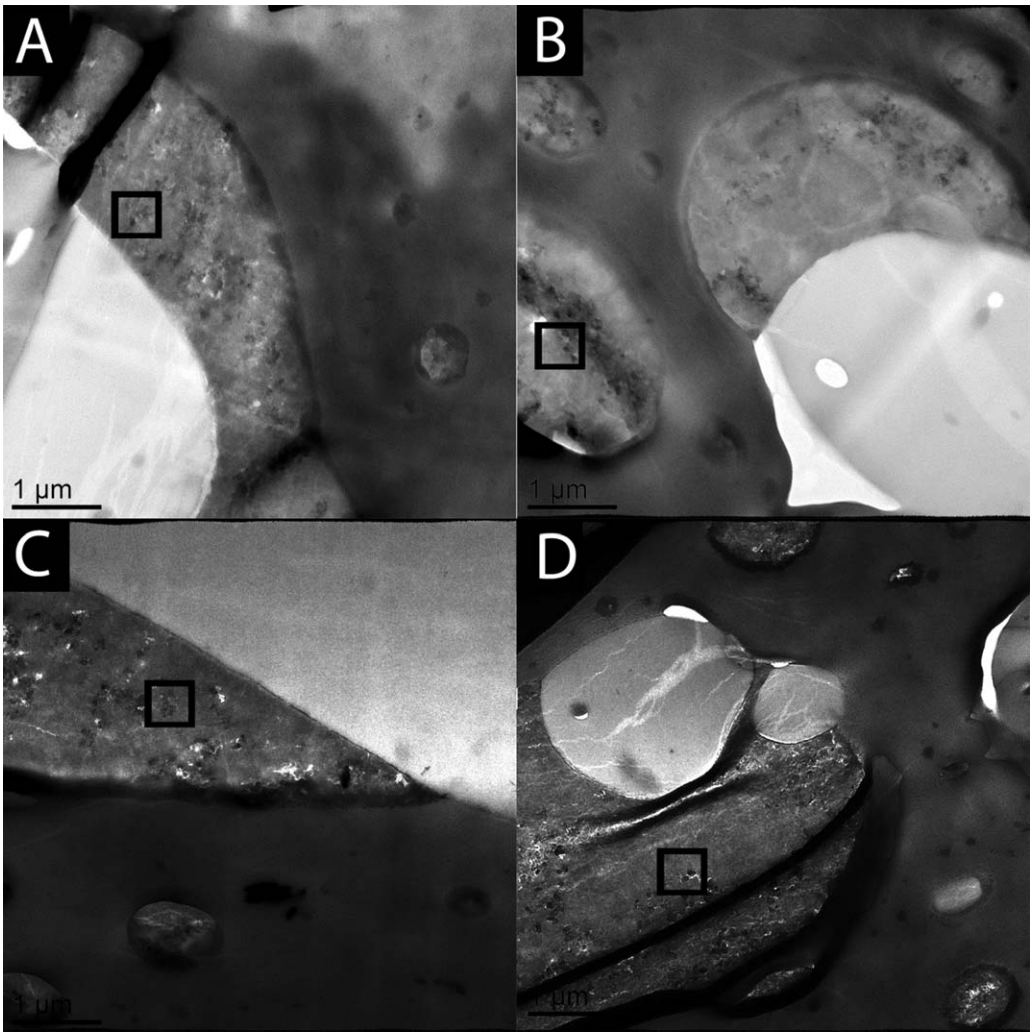

Figure 7. TEM images at 4000× of PP/PMMA/(EAA–CB) annealed for (A) 6 min and (C) 150 min, and PP/PMMA/EAA/CB annealed for (B) 6 min and (D) 150 min. CB (~20 nm dark spots—see black boxes for example) is only found in the EAA phase independent of the composition or anneal time.

that the PP/PMMA/EAA/CB is slightly higher (inset to Figure 1), which may be attributed to poorer dispersion in PP/PMMA/EAA/CB due to omission of a CB masterbatch step. The resistivities after annealing for 150 min were found to be approximately an order of magnitude lower than the samples annealed for 30 min (Figure 1), indicating that at least 150 min annealing is needed to reach equilibrium by this method.

Gubbels *et al.*[15] suggested that CB particles migrate to the interface by transferring from the phase with lowest affinity to that of highest affinity and preferentially interacting with that phase taking advantage of the temporary state where they are blocked and accumulate at the interface, which was deemed kinetic control. The authors also suggested thermodynamic control if the surface affinity of the particles is balanced with that of the two polymers in a binary blend, in which case they will be thermodynamically stabilized at the interface regardless of the processing technique. Some proposed mechanisms by which particles transfer from one phase to the other pass the interface or more generally move inside the polymer blend in the molten state are discussed elsewhere.[26] It is evident from

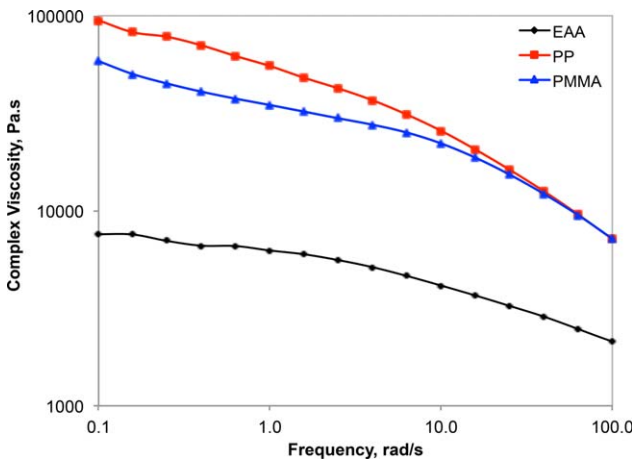

Figure 8. Complex viscosity of the pure PP, PMMA, and EAA polymers at 190°C. [Color figure can be viewed in the online issue, which is available at wileyonlinelibrary.com.]

Table IV. Viscosity Ratio of the PP and PMMA Major Components (50/50 vol %) as a Function of Frequency

Frequency (rad/s)	Viscosity ratio
100	1.0
10	1.2
1	1.6
0.1	1.6

this study that the compounding sequence and especially the thermal annealing times are critical for the formation of efficient conductive networks in this polymer system. The resistivities were exceedingly high after experiencing intensive shear mixing in the initial melt compounding step followed by 6 min of annealing. However, after annealing for 30 min low levels of resistivity were achieved, representing more than three orders of magnitude change.

Resistivity as a Function of Temperature. The effect of temperature on the resistivity is associated with various factors including the types of polymers and fillers, the polymer melt points, the structure of the conductive network, CB content, melt mixing conditions, and CB chemical treatment.[26] Figure 2 shows the stability of the resistivity over time at 160°C for the multiphase composites that had first been annealed for 30 min at 190°C. There was little change in the resistivity over time at 160°C, though after an initial small decrease a small increase was observed after 16 h. This stability at 160°C, which is well above likely use temperatures for polyolefin composites, is valuable from a practical end-use and application standpoint.

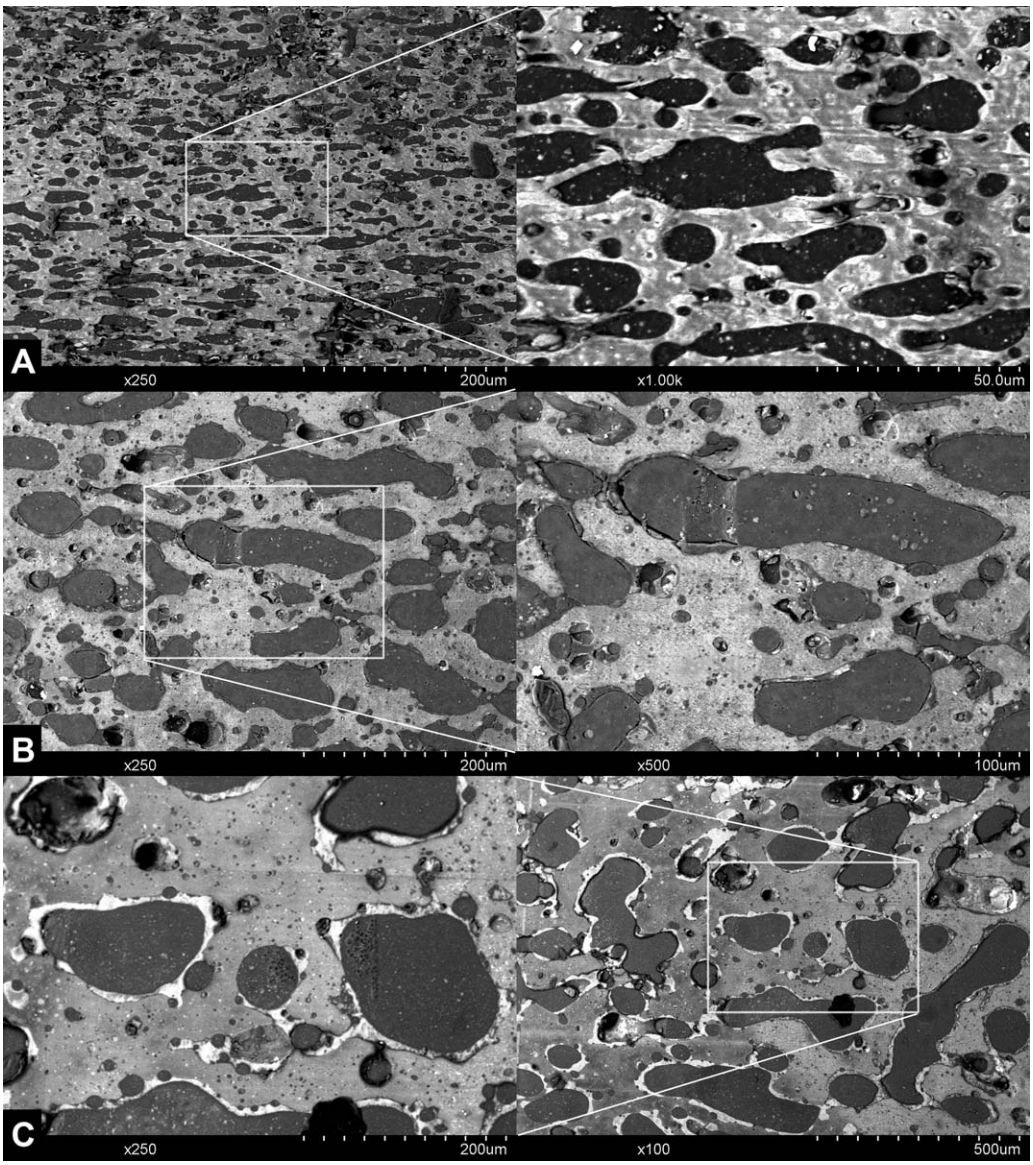

Figure 9. SEM images of PP/PMMA/(EAA–CB) annealed for (A) 6 min, (B) 30 min, and (C) 150 min. Left column shows images for each annealing time at the same (250×) magnification. Right column shows higher (A,B) and lower (C) magnification images to show more details.

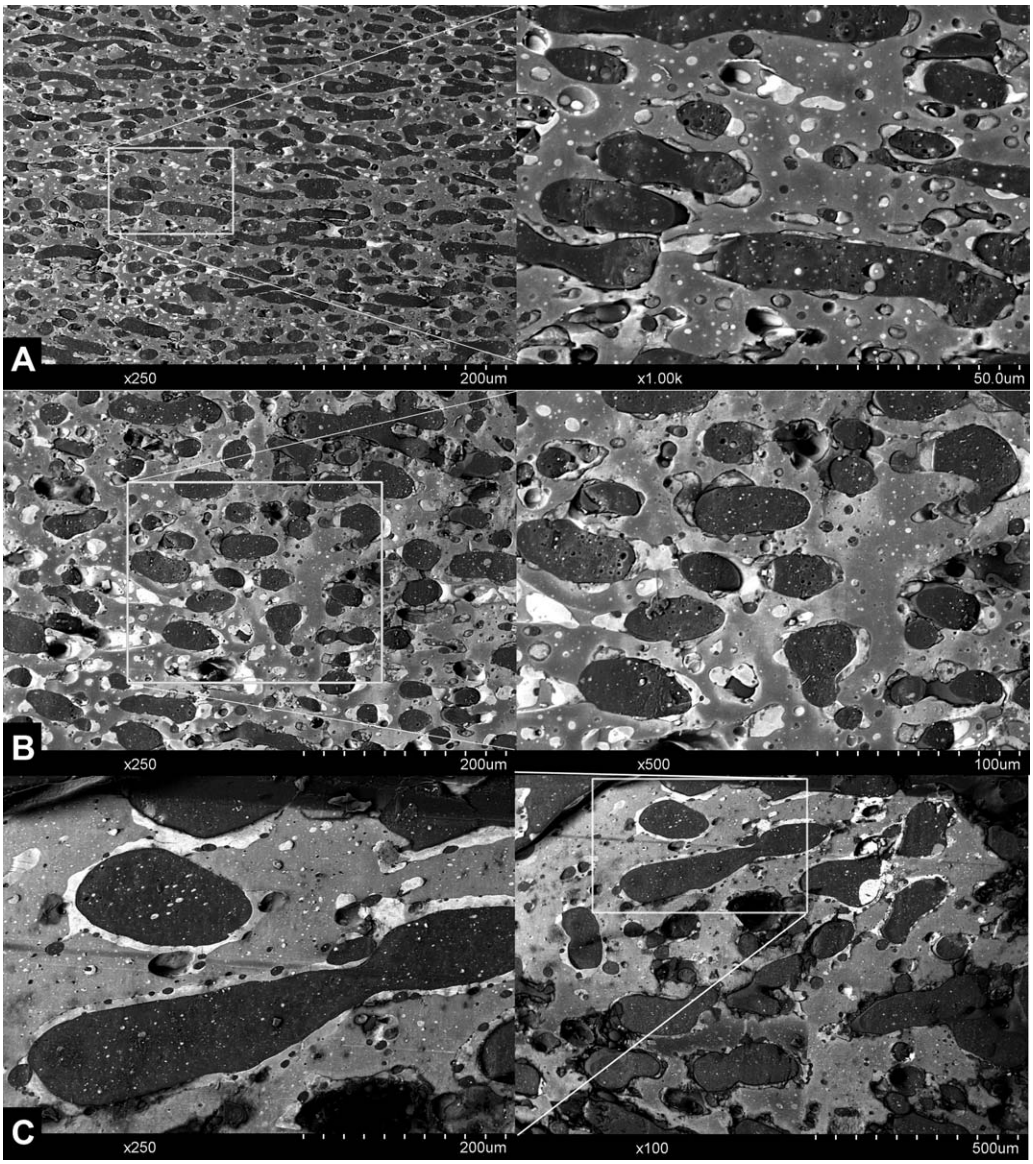

Figure 10. SEM images of PP/PMMA/EAA/CB annealed for (A) 6 min, (B) 30 min, and (C) 150 min. Left column shows images for each annealing time at the same (250×) magnification. Right column shows higher (A, B) and lower (C) magnification images to show more details.

Additional Characterization

DSC thermograms provide a qualitative measure to determine if polymer blends are miscible or immiscible. DSC curves were obtained for the individual polymers and the PP/PMMA/(EAA–CB) ternary polymer blend composite in the temperature range of −50 to 220°C shown in Figure 3. Single melting peaks were observed at 97.5 and 163.4°C for the semicrystalline EAA and PP, respectively. The PMMA is an amorphous polymer with a glass transition temperature observed at 96.7°C. As expected for the immiscible polymer blend, two distinct melting peaks were observed at 97.6 and 161.4°C for the PP/PMMA/(EAA–CB) composite characteristic of the EAA and PP melt points. The PMMA glass transition in the composite was masked by the crystalline melt point of the EAA.

Rheology has been used for assessing filler dispersion in polymer melts.[27] Dynamic oscillatory shear was used to characterize the PP/PMMA/EAA composites in an attempt to gain insight into the CB migration and distribution as a function of annealing time and compounding sequence. However, differences in complex viscosities and storage moduli among the composites at the same annealing times were quite small and not considered to show statistically significant differences regardless of the compounding sequence.

Morphology

Localization of CB Filler. The selective localization and dispersion state of CB particles in a polymer blend can be predicted qualitatively from the value of the wetting coefficient and minimizing the interfacial free energy in Young's equation described elsewhere.[7,22,28] In this study, SEM and TEM were used to characterize the phase morphology of the polymer composites and distribution of CB as a function of compounding sequence and annealing time at 190°C. Of the three polymer phases in the

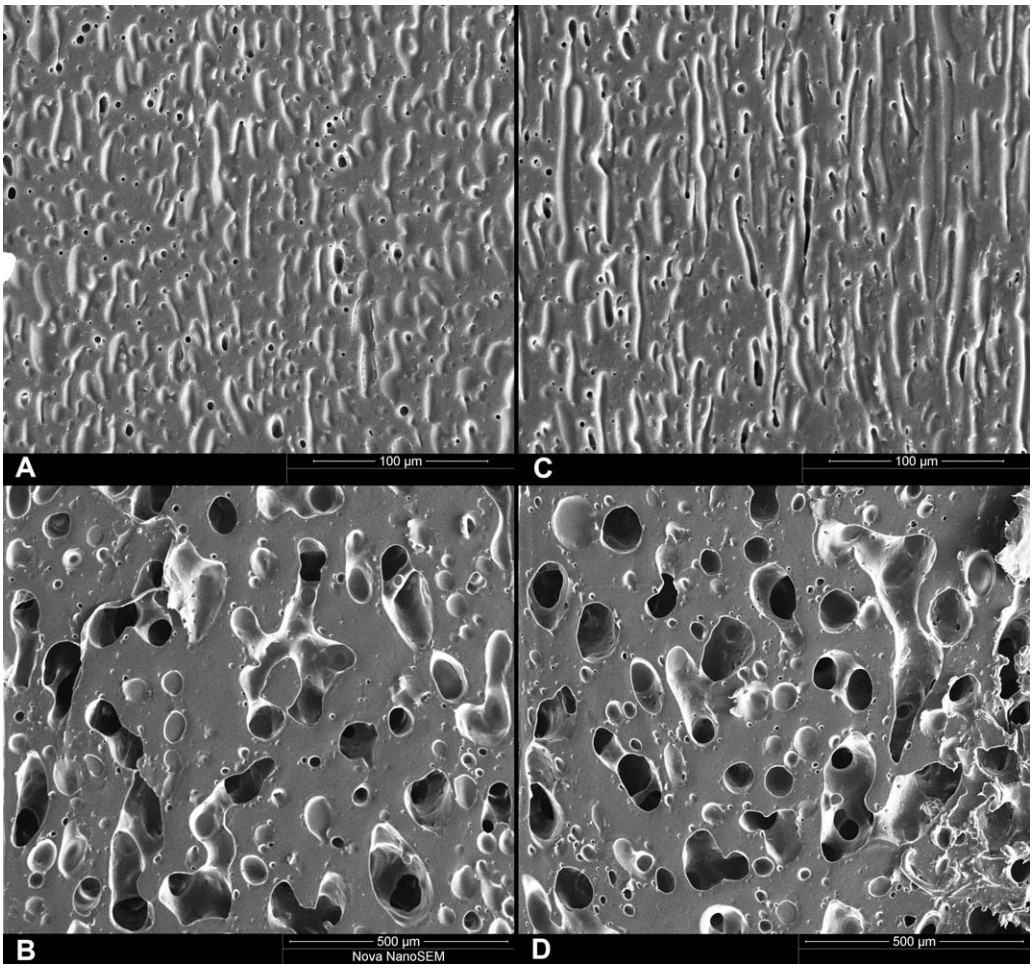

Figure 11. SEM images of etched samples of PP/PMMA/(EAA–CB) annealed for (A) 6 min and (B) 150 min, and PP/PMMA/EAA/CB annealed for (C) 6 min and (D) 150 min.

system, the EAA picks up the most stain allowing a view of the semicrystalline (see the gray rectangle in Figure 4) structure in the phase. The PMMA picks up the least stain and so remains the second brightest object in the TEM images (the brightest being any holes in the film) with no discernible structure. The PP picks up stain more than the PMMA, which is hypothesized to be a result of the lower density of the polymer, and is the second darkest object in the images (the darkest being folds or overlapping sections of the film). Thus, the overall contrast from darkest to brightest is folds > EAA > PP > PMMA > holes. TEM images were taken at 1000× and 20,000× with the intention of showing, primarily, which phases contained the CB, and secondarily, as many of the three phases present as possible (see Figures 5 and 6).

The CB can be identified in the TEM images as small nodular particles that have a dark edge and a lighter inside (see the black and white boxes in Figure 4). In all the samples, even those annealed for 6 min, the CB is within the EAA phase (see black boxes in Figure 7). No CB was observed in the PP or PMMA phases in any of the samples. Consequently, the continuity of the EAA phase is anticipated to be the primary factor controlling the resistivity.

Evolution of Tri-Continuous Phase Morphology. Empirical and semiempirical models have been developed over the last three decades to estimate the phase inversion composition in terms of material properties and processing conditions.[29,30] Paul and Barlow[14] proposed that the critical condition for phase inversion from a sea-island microstructure to co-continuous structure is determined by the viscosity ratio in eq. (1):

$$\frac{\phi_1}{\phi_2} \times \frac{\eta_2}{\eta_1} = X, \tag{1}$$

where ϕ is the volume fraction and η is the melt viscosity of phase 1 or phase 2. Phase continuity may be predicted by the Jordhamo relationship where:[31]

$X > 1$, Phase 1 is continuous

$X \approx 1$, Dual phase continuity or phase inversion

$X < 1$, Phase 2 is continuous

Therefore, an increase in the volume fraction or decrease in melt viscosity of the minor component would lead to matrix continuity to enable electrical conductivity.

As compared to the previous work, different grades of PP and EAA polymers were used. Therefore, the viscosities for the pure polymer components were measured as a function of frequency

at 190°C (Figure 8) to predict the influence of the viscosity ratio on the polymer blend phase morphology. The viscosity ratio as a function of frequency for 50/50 vol % split of the PP and PMMA major phases (each present at 42 vol % in the overall composition) are listed in Table IV. All of viscosity ratios are close to 1, predictive of phase inversion and co-continuity according to the Jordhamo relationship. Analogously, the minor component EAA would be predicted to spread in the interphase due to a low viscosity compared to the PP and PMMA phases.

Figures 9 and 10 are back-scattered SEM images of PP/PMMA/(EAA–CB) and PP/PMMA/EAA/CB, respectively. In these images the PMMA appears dark and the PP is the lighter continuous phase. The EAA is the minor component, and in most regions is much lighter than the other two phases due to the staining of the EAA with the RuO_4. In some areas the staining appears less distinct, suggesting the samples did not stain uniformly, but the three phases are still discernible.

In both the PP/PMMA/(EAA–CB) and PP/PMMA/EAA/CB the same progression in morphology with annealing is observed. The initial samples [Figures 9(A) and 10(A)] show a fine dispersion of PMMA domains in a continuous PP matrix. The EAA is mostly dispersed within the PP phase as discrete, roughly spherical domains. On annealing [Figures 9(B,C) and 10(B,C)] the morphology changes substantially. The PP remains a continuous matrix while the PMMA phases coalesce to form substantially (almost two orders of magnitude) larger domains. The most striking change is in the EAA morphology, which goes from being mostly dispersed in the PP matrix as discrete, noncontiguous spheres to being almost entirely at the PP–PMMA interface and, in many areas, bridging between adjacent PMMA domains. Solvent etching with THF was used to dissolve and remove the PMMA to better delineate the three-dimensional structures. SEM images of etched cross-sectioned faces of the PP/PMMA/(EAA–CB) and PP/PMMA/EA/CB samples after 6 and 150 min annealing were obtained (Figure 11). For both samples the 6 min annealing shows that the majority of PMMA domains are discrete and do not show interconnectivity into the sample. However, in the 150 min annealed samples the PP phase is intact and continuous while channels into the bulk can be seen, indicating that the PMMA phase is also continuous demonstrating tri-continuity.

CONCLUSIONS

Previous work has identified PP/PMMA/EAA/CB as very efficient conductive composites due to triple percolation. In this study, it was demonstrated that kinetic and thermodynamic parameters influenced polymer blend phase morphology and localization of filler to increase electrical conductivity as a function of annealing time. The conductivity was found to be kinetically driven during the intensive compounding process, and was dependent on the mode of addition of CB. Upon annealing, the morphology and conductivity underwent rapid transitions.

Though statistically significant differences remained after 30 min of annealing, by 150 min the conductivities were the same, within experimental error, for all modes of CB addition suggesting a transition from kinetic to thermodynamic control after long annealing times. The resistivity after annealing for 150 min was found to be lower by a statistically significant amount compared to the samples annealed for 30 min.

The overall increase in conductivity upon annealing was determined to be the result of changes in the phase morphology. In particular, the EAA phase goes from being mostly dispersed in the PP matrix as discrete, noncontiguous spheres to being almost entirely at the PP–PMMA interface, forming a tri-continuous morphology. The evolution of conductivity upon annealing is attributed to this rather than to changes in localization of CB, given that the CB was found to be entirely located in the EAA phase even at short annealing times (and independent of compounding sequence), where the conductivity was not measurable. No CB was observed in the PP or PMMA phases. The conductivity enhancement was only observed at longer annealing times after formation of a tri-continuous phase morphology, which was confirmed by solvent etching. The addition of CB via masterbatch results in significantly lower resistivity compared to when added direct to the system during compounding after 30 min annealing by a statistically significant amount.

ACKNOWLEDGMENTS

The authors are thankful to The Dow Chemical Company for the support of this research. They are greatly indebted to the reviewers for their helpful comments and suggestions.

REFERENCES

1. Strumpler, R.; Glatz-Reichenbach, J. *J. Electroceram.* **1999**, *3*, 329.
2. Bartnikas, R.; Srivastava, K. D. Power and Communication Cables: Theory and Applications; IEEE Press: New York, **2000**.
3. Huang, J.-C.; Shen, H.-F.; Chu, Y.-T. *Adv. Polym. Technol.* **1994**, *13*, 49.
4. Levon, K.; Margolina, A.; Patashinsky, A. Z. *Macromolecules* **1993**, *26*, 4061.
5. Tchoudakov, R.; Breuer, O.; Narkis, M.; Siegmann, A. *Polym. Eng. Sci.* **1997**, *37*, 1928.
6. Zhang, Q.-H.; Chen, D.-J. *J. Mater. Sci.* **2004**, *39*, 1751.
7. Brigandi, P. J.; Cogen, J. M.; Pearson, R. A. *Polym. Eng. Sci.* **2014**, *54*, 1.
8. Feng, J.; Chan, C.-M. *Polym. Eng. Sci.* **1998**, *38*, 1649.
9. Tchoudakov, R.; Breuer, O.; Narkis, M.; Siegmann, A. *Polym. Eng. Sci.* **1996**, *36*, 1336.
10. Sumita, M.; Sakata, K.; Hayakawa, Y.; Asai, S.; Miyasaka, K.; Tanemura, M. *Colloid Polym. Sci.* **1992**, *270*, 134.
11. Cui, L.; Zhang, Y.; Zhang, Y.; Zhang, X.; Zhou, W. *Eur. Polym. J.* **2007**, *43*, 5097.
12. Wu, S. Polymer Interface and Adhesion; Marcel Dekker: New York, **1982**.
13. Hobbs, S. Y.; Dekkers, M. E. J.; Watkins, V. H. *Polymer* **1988**, *29*, 1598.

14. Paul, D. R.; Barlow, J. W. *J. Macromol. Sci. Rev. Macromol. Chem.* **1980**, *C18*, 109.
15. Gubbels, F.; Jerome, R.; Vanlathem, E.; Deltour, R.; Blacher, S.; Brouers, F. *Chem. Mater.* **1998**, *10*, 1227.
16. Virgilio, N.; Marc-Aurele, C.; Favis, B. D. *Macromolecules* **2009**, *42*, 3405.
17. Al-Saleh, M. H.; Sundararaj, U. *Compos. Part A* **2008**, *39*, 284.
18. Al-Saleh, M. H.; Sundararaj, U. *Eur. Polym. J.* **2008**, *44*, 1931.
19. Al-Saleh, M. H.; Sundararaj, U. *Polym. Eng. Sci.* **2009**, *49*, 693.
20. Lu, C.; Hu, X.-N.; He, Y.-X.; Huang, X.; Liu, J.-C.; Zhang, Y.-Q. *Polym. Bull.* **2012**, *68*, 2071.
21. Lu, C.; Liu, C.-Y.; Li, Z.-Z.; Jiang, T.; Liu, J.-C.; Peng, S.-G.; Zhang, Y.-Q. *Chin. J. Polym. Sci.* **2010**, *28*, 869.
22. Shen, L.; Wang, F.; Jia, W.; Yang, H. *Polym. Int.* **2012**, *61*, 163.
23. Gubbels, F.; Blacher, S.; Vanlathem, E.; Jerome, R.; Deltour, R.; Brouers, F.; Teyssie, P. *Macromolecules* **1995**, *28*, 1559.
24. Xu, H. P.; Bing, N. C.; Wu, Y. H.; Yang, D. D.; Dang, Z. M. *Mater. Res. Soc. Symp. Proc.* **2010**, *1269E*, 1269.
25. Zhou, P.; Yu, W.; Zhou, C.; Liu, F.; Hou, L.; Wang, J. *J. Appl. Polym. Sci.* **2007**, *103*, 487.
26. Yu, G.; Zhang, M. Q.; Zeng, H. M. *J. Appl. Polym. Sci.* **1998**, *70*, 559.
27. Zhu, J.; Wei, S.; Yadav, A.; Guo, Z. *Polymer* **2010**, *51*, 2643.
28. Sumita, M.; Sakata, K.; Asai, S.; Miyasaka, K.; Nakagawa, H. *Polym. Bull.* **1991**, *25*, 265.
29. Miles, I. S.; Zurek, A. *Polym. Eng. Sci.* **1988**, *28*, 796.
30. Omonov, T. S.; Harrats, C.; Moldenaers, P.; Groeninckx, G. *Polymer* **2007**, *48*, 5917.
31. Jordhamo, G. M.; Manson, J. A.; Sperling, L. H. *Polym. Eng. Sci.* **1986**, *26*, 517.